Supporting Information

Koven et al. 10.1073/pnas.1103910108

SI Text

Model and Experimental Setup. The vertical discretization of soil temperature and soil carbon in this version of ORCHIDEE uses a 32-layer exponential grid, with a maximum depth of 51.2 m. At each timestep, soil carbon is input from a fraction of decomposed litter following standard ORCHIDEE (1), and vertically discretized to an exponential profile with e-folding depth based on the plant functional type-specific rooting depth profile. Where permafrost layers exist, soil carbon inputs are set to zero below the permafrost table, and the total profile is adjusted so that the integral of carbon inputs to the active layer is conserved. The temperature-dependant soil carbon residence time is based on the standard ORCHIDEE scheme, which follows the CENTURY model (2), except that it is calculated separately for each soil layer based on the temperature at that layer.

For the Arctic region, we assume that temperature is the dominant physical control on decomposition (3, 4), and thus the only moisture limitations to soil carbon respiration are those that accompany freezing. For the freeze and subsequent experiments, we parameterize the liquid moisture control on decomposition by modifying the temperature dependence of respiration in frozen soils. Respiration thus becomes lower than in our control case, in which we use only a constant Q_{10} of 2 throughout the temperature range. A variety of frozen respiration functions have been proposed (5, 6), for example spanning Q_{10} range from 10^2 to 10^6 (5). Here we perform four separate sensitivity experiments (Fig. S2): two with a second exponential with Q_{10} values and two with a linear drop off between the fixed respiration rate at 0 °C and a T_{crit} where respiration goes to 0. For the Q_{10} experiments, we use Q_{10} of 100 and 1,000 for temperatures below 0 °C; for the T_{crit} experiments, we use T_{crit} values of −1C and −3C. We report the mean and standard deviation of all four sets of runs for the freeze experiment; for the heating, and permafrost experiments we use a T_{crit} of −1C.

For the permafrost experiment, we perform a sensitivity test to the vertical diffusion constant that we use to model processes such as cryoturbation that transport organic material from surface or active layer into the permafrost layers of the soil. The rate of such diffusion is poorly known, however radiocarbon dates of subducted organic material (7) suggest a centennial to millennial timescale. Thus we try to bracket this range, with diffusion constants of 1 e–2 m^2/y and 1 e–3 m^2/y.

For the heating experiment, we also try to bracket the range of potential values for the exothermic heat release term described by Khvorostyanov et al. (8). We implicitly use a value of zero for all prior experiments (control, freeze, and permafrost); for the heating experiment, we additionally test the model with values of 20 and 40 MJ/kg C, which covers the range used by Khvorostyanov et al. (8).

The surface carbon stocks are initialized iteratively for 10,000 y as described by Koven et al. (9). For the simulations that involve permafrost carbon, i.e. permafrost and heating, we also include carbon in deeper soil layers where yedoma soils exist in Eastern Siberia. We define the yedoma geographic extent following Walter et al. (10); we use initial yedoma carbon concentrations of 17.6 Kg C/m^3 following Zimov et al. (11) and a bulk lability set by partitioning the yedoma carbon between the three ORCHIDEE carbon lability pools to match the carbon residence time of the 5 °C soil incubation data of Dutta et al. (12).

Mean and error estimates for the freeze, permafrost, and heating experiments are found as the mean and standard deviation of an ensemble of model runs with varied parameter values. For each ensemble member, a chosen parameter value is used in the initial model equilibration and for the subsequent transient experiments (control, CO_2-only, CO_2+climate). For the freeze experiment, we vary the frozen respiration function; for the permafrost experiment, we vary the soil organic matter (SOM) vertical diffusion constant; and for the heating experiment, we vary the exothermic heat per unit carbon consumption term.

Comparison of modeled and observed carbon stocks. A strong difference between the experiments tested here is seen in the size of the carbon stocks that are initially in equilibrium with the model (Fig. S4 and Table S1), where inclusion of the freeze-induced inhibition of respiration leads to larger equilibrium soil carbon stocks and brings the model in closer agreement with inventories of high-latitude soil carbon in the northern circumpolar soil carbon database (NCSCD) (13). This increase in SOM C stocks is particularly true in the Eastern Siberian region, where high carbon stocks are associated with cryoturbated permafrost-affected soils (turbels). Because peat formation processes are not included in ORCHIDEE, we strongly underestimate the substantial carbon stocks associated with peat deposits, particularly those in western Siberia and Canada.

The large increase in initial high-latitude soil C stocks (from ∼200 Pg to ∼500 Pg C in the top 3 m of soil) demonstrates the large sensitivity of ecosystem carbon storage to the representation of soil processes in the model, despite these effects having only a weak influence on the behavior of the modeled carbon fluxes on interannual-to-seasonal timescales due to the slow response time of the soil C pool.

Sensitivity of results to model parameters and processes. For the ensemble of runs performed with different frozen respiration functions, initial carbon stocks ranged 246 to 264 for the top 1 m of soils, with larger carbon stocks associated with lower frozen respiration rates. Lower respiration rates also translated to higher sensitivity of the carbon pools to warming, with a standard deviation of 3 Pg between the ensemble members.

For the permafrost experiment, we vary the vertical diffusion constant by an order of magnitude. For the faster diffusion case ($k = 10^{-2}$ m/y), total carbon stocks are larger than the slower diffusion case ($k = 10^{-3}$ m^2/y) after the initial 10,000 y spin up period due to faster equilibration between the active layer carbon and permafrost carbon. In addition, the lability of the permafrost carbon was higher, with a higher proportion of active pool to slow pool carbon in the permafrost layers. This increased lability leads to a higher vulnerability of the permafrost carbon stocks to warming, and thus higher loss rates (69 Pg vs. 55 Pg, respectively).

For the permafrost experiment, deeper carbon stocks act as only a weak source of methane (approximately 1 Tg/y), because the grid cells with yedoma are only in the coldest parts of Siberia, which do not completely thaw during the time horizon considered here. Shallower permafrost carbon does not act as a strong methane source; because we assume here that only the active carbon pool is available as a substrate for methanogenesis, the residence time of this carbon is short relative to its mixing time by cryoturbation, and thus the stock of this pool is minor relative to the wetland sources.

We perform two scenarios with nonzero values of the microbial heat release term: 20 MJ/kg C and 40 MJ/kg C. The overlap with the error shading in Fig. 2*B* between the lower range of the heating case and the upper range of the permafrost case is due to the fact that the middle estimate of the microbial heat release

parameter leads to only a minor change in the model behavior, it is only the upper estimate, in which the heat released is enough to lead to further thaw of deeper permafrost, that large carbon emissions occur.

Our results also show that the heat release from organic carbon decomposition can increase both the CO_2 and CH_4 release. The idea of microbial heat release playing a role in permafrost carbon cycling was first proposed in ref. 14. This idea has strong theoretical justification—in that thermodynamics dictates that the energy differential between organic substrate and inorganic carbon will eventually become thermal energy—and is supported by some field evidence (15). The actual quantity of heat released per unit carbon respired (H) is not well constrained (here we vary H between 0 and 40 MJ/kg C) (8), and more investigation is needed to determine the strength of this mechanism in actual permafrost soils. In particular, this mechanism has a very weak effect on the steady-state dynamics of the model (Fig. S4); instead it only becomes important when the system is perturbed out of equilibrium. Thus we cannot reject the hypothesis that microbial heat production could affect the carbon balance, as obtained in local field experiments (15). However, we note that the heating process has a strong threshold behavior relative to the heat release parameter H, (8) and only acts to create a significant extra source of CO_2 if the parameter H is above 20 MJ/kg C. Therefore, this process will only be important if the heat release is at the upper end of what is thermodynamically possible, and in this case the model present-day carbon balance falls out of agreement with estimates of the high-latitude carbon balance; because of the strong threshold behavior, lack of quantitative observations at the appropriate scale, and overall large uncertainty of this process, we instead consider the permafrost case, which does not include the heating term, our best estimate.

The large source of CO_2 and CH_4 that results from climate change in the model experiment with the upper estimate of microbial heat decomposition is qualitatively similar to that described by Khvorostyanov et al. (8): In certain grid cells, the heat released results in a positive feedback that leads to thawing to the base of the C-rich soil (25 m). In reality, however, the impact of a biological heat source in soils may be quite different. A particular simplification inherent in this modeling framework is that we model heat transfer as 1-D heat conduction; real soils will have 3-D heat transport, and advection of heat by groundwater and vapor flow may be critical to the thawing processes (16). However, although these processes may damp any positive feedback loops such as the one we calculate here for the microbial heat release experiment, they may also act to destabilize and accelerate thaw through processes such as thermokarst.

The wetland CH_4 results are calculated with the ORCHIDEE-WET model (17, 18), separately, forced by the same scenario, and added to the CH_4 emissions from the permafrost model. The CH_4 submodel of ORCHIDEE-WET is based on the Walter et al. (19) CH_4 model, in which methanogenesis, methanotrophy, and CH_4 transport are calculated for saturated soil columns (17, 18) The temperature sensitivity of methanogenesis for a given substrate availability in Walter et al. (19) and ORCHIDEE-WET is based on a modified Q_{10} formulation:

$$g = f(T(t,z))Q_{10}^{T(t,z)-T_{\text{mean}}}, \qquad \textbf{[S1]}$$

where $f(T)$ is a step function that halts methanogenesis in frozen soils, and the term T_{mean} is the location-dependant mean annual temperature. In the original Walter et al. (19) formulation, Q_{10} was set to 6; here it is set to 3 based on an optimization of the model at several sites and against global inversions, as described by Ringeval et al. (17). In addition, we test alternate hypotheses about microbial adaptation to climate change to assess the uncertainty associated with adaptation to climate change, by allowing T_{mean} to vary or stay fixed.

In addition to the sensitivity to T_{mean}, the wetland CH_4 model is run with separate experiments allowing the soil C (which is used as a proxy for the methanogenesis substrate) to evolve with time, and held constant at preindustrial values (Table S2). Similarly, separate varying and constant experiments are done with the modeled wetland extent. The results demonstrate a high sensitivity of the model to these processes, with multiple local feedback mechanisms, including a sensitivity of the wetland fraction to transpiration fluxes via both CO_2 fertilization and climate change. More discussion of these mechanisms is in ref. 18.

1. Krinner G, et al. (2005) A dynamic global vegetation model for studies of the coupled atmosphere-biosphere system. *Global Biogeochem Cycles* 19:GB1015.
2. Parton W, Stewart J, Cole C (1988) Dynamics of C, N, P, and S in grassland soils—a model. *Biogeochemistry* 5:109–131.
3. Hobbie SE, Schimel JP, Trumbore SE, Randerson JR (2000) Controls over carbon storage and turnover in high-latitude soils. *Glob Change Biol* 6:196–210.
4. Goulden M, et al. (1998) Sensitivity of boreal forest carbon balance to soil thaw. *Science* 279:214–217.
5. Monson R, et al. (2006) Winter forest soil respiration controlled by climate and microbial community composition. *Nature* 439:711–714.
6. Mikan CJ, Schimel JP, Doyle AP (2002) Temperature controls of microbial respiration in arctic tundra soils above and below freezing. *Soil Biol Biochem* 34:1785–1795.
7. Kaiser C, et al. (2007) Conservation of soil organic matter through cryoturbation in Arctic soils in Siberia. *J Geophys Res (Biogeosci)* 112:G02017.
8. Khvorostyanov D, Krinner G, Ciais P, Heimann M, Zimov S (2008) Vulnerability of permafrost carbon to global warming. Part I: Model description and role of heat generated by organic matter decomposition. *Tellus Ser B* 60:250–264.
9. Koven C, et al. (2009) On the formation of high-latitude soil carbon stocks: The effects of cryoturbation and insulation by organic matter in a land surface model. *Geophys Res Lett* 36:L21501.
10. Walter KM, Edwards ME, Grosse G, Zimov SA, Chapin FS, III (2007) Thermokarst lakes as a source of atmospheric CH_4 during the last deglaciation. *Science* 318:633–636.
11. Zimov S, et al. (2006) Permafrost carbon: Stock and decomposability of a globally significant carbon pool. *Geophys Res Lett* 33:L20502.
12. Dutta K, Schuur EAG, Neff JC, Zimov SA (2006) Potential carbon release from permafrost soils of Northeastern Siberia. *Glob Change Biol* 12:2336–2351.
13. Tarnocai C, Swanson D, Kimble J, Broll G (2007) Northern Circumpolar Soil Carbon Database. (Research Branch, Agriculture and Agri-Food Canada, Ottawa).
14. Zimov S, et al. (1996) Siberian CO_2 efflux in winter as a CO_2 source and cause of seasonality in atmospheric CO_2. *Clim Change* 33:111–120.
15. Zimov SA, et al. (2006) Permafrost carbon: Stock and decomposability of a globally significant carbon pool. *Geophys Res Lett* 33:L20502.
16. Kane D, Hinkel K, Goering D, Hinzman L, Outcalt S (2001) Nonconductive heat transfer associated with frozen soils. *Global Planet Change* 29:275–292.
17. Ringeval B, et al. (2010) An attempt to quantify the impact of changes in wetland extent on methane emissions on the seasonal and interannual time scales. *Global Biogeochem Cycles* 24:GB2003.
18. Ringeval B, et al. (2011) Climate-methane feedback from wetlands and its interaction with the climate-carbon cycle feedback. *Biogeosci Discuss* 8:3203–3251.
19. Walter B, Heimann M, Matthews E (2001) Modeling modern methane emissions from natural wetlands I. Model description and results. *J Geophys Res (Atmos)* 106:D24.

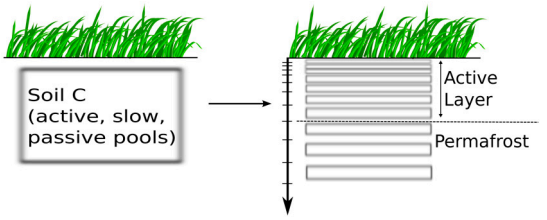

Fig. S1. Schematic of model structure: Vertically integrated soil C pools have been replaced by an explicit vertical discretization of soil carbon, and coupling with permafrost dynamics. In the freeze and subsequent experiments, soil carbon turnover time is dramatically increased in frozen soil layers. In the permafrost experiment, soil carbon is mixed from the active layer into permafrost layers during spin up, leading to a buildup of soil carbon in frozen layers.

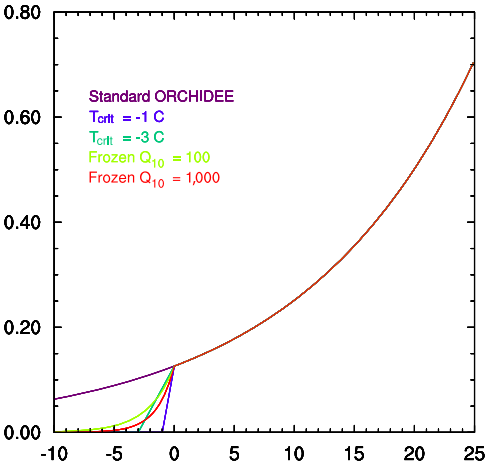

Fig. S2. Modeled frozen respiration functions. All follow the standard ORCHIDEE respiration control function ($Q_{10} = 2$) for unfrozen soils; two curves follow a second exponential function ($Q_{10} = 100, 1,000$) for frozen soils, and two use a linear drop off to zero respiration at a temperature $T_{crit} = -1$ or -3 C.

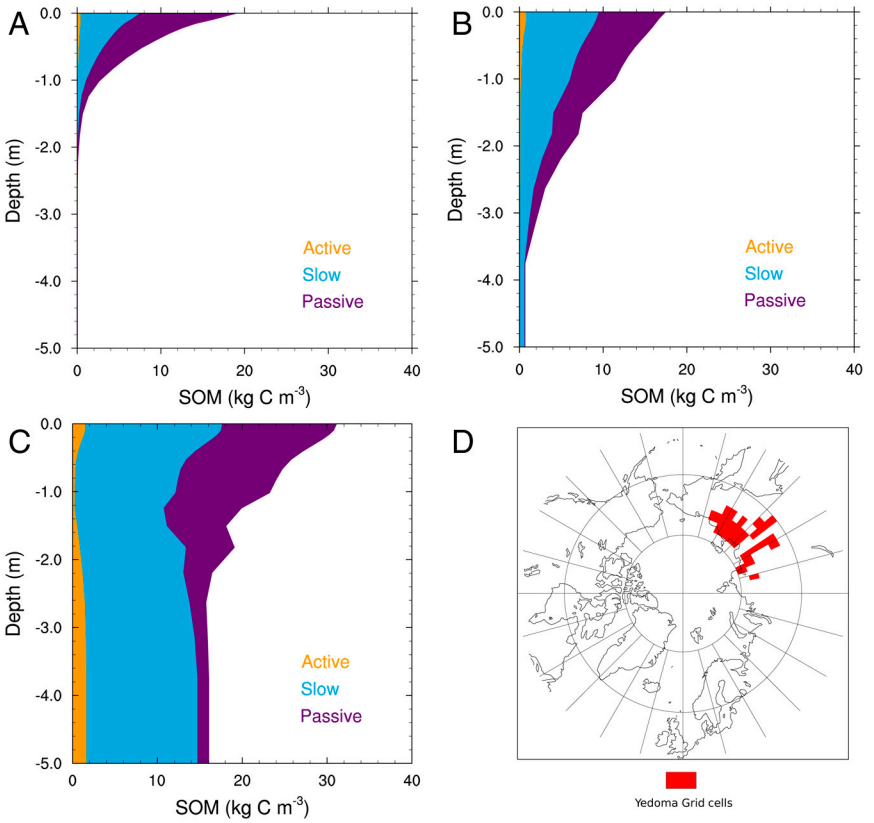

Fig. S3. Modeled soil C vertical profiles. (*A*) Mean over all permafrost grid cells in freeze case. (*B*) Mean over permafrost grid cells in permafrost case. (*C*) Mean over all yedoma grid cells in permafrost case. (*D*) Map of grid cells where yedoma is initialized to be present.

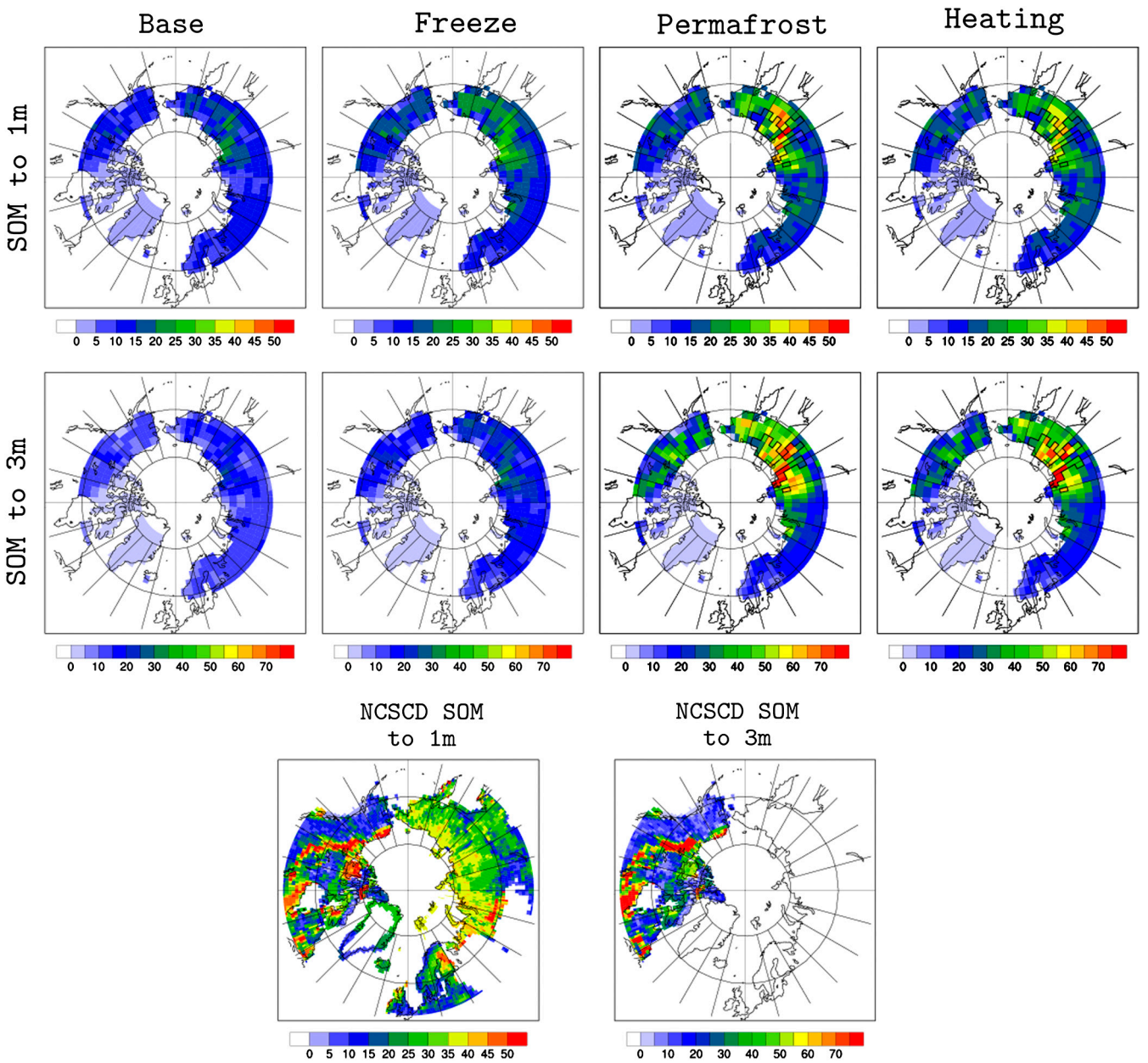

Fig. S4. Maps of initial soil carbon (kg C/m2) to depths of 1 m and 3 m for each experiment, and for comparison, observations from the NCSCD (13). Outlined grid cells in permafrost and heating experiments are those where yedoma carbon stocks are present in model.

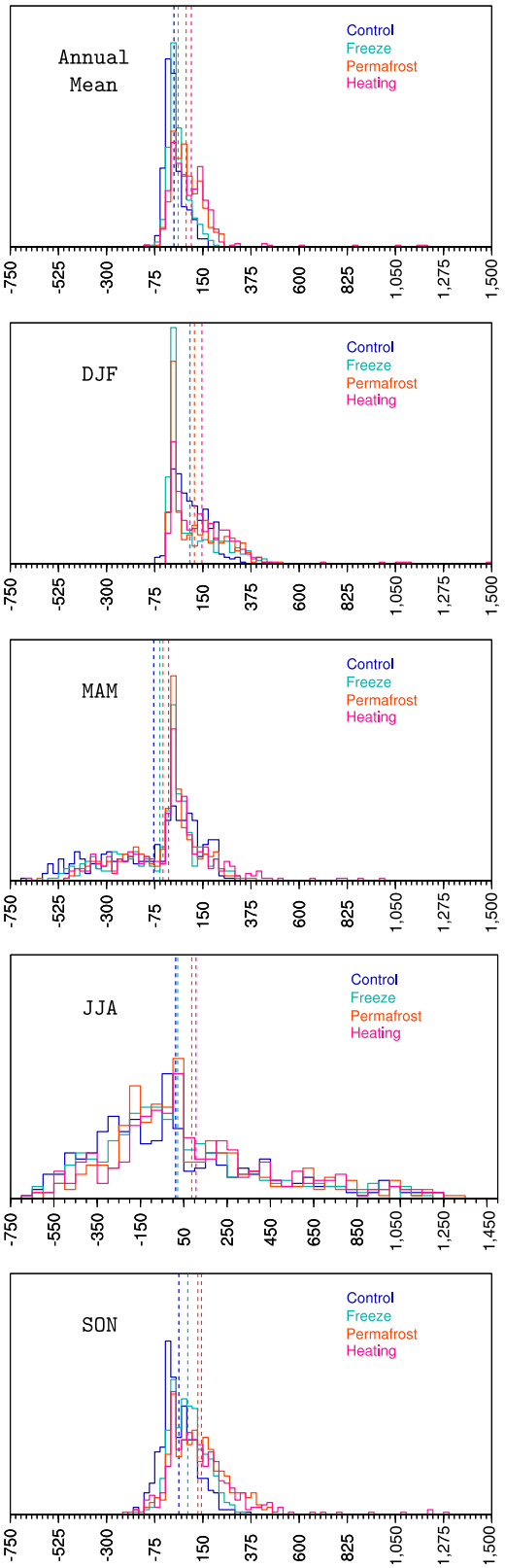

Fig. S5. Histograms of CO_2 balance for each case at the end of the modeled period (gC/m2/y), for annual mean and for each season.

Table S1. List of experiments presented here, with description of processes added in each experiment, parameter ranges tested, and total CO_2 flux resulting from climate change alone at end of each experiment

Experiment Name	Processes included	Parameters varied and range tested	Initial soil carbon stock for region north of 60°N to 1 m (Pg)	Initial soil carbon stock for region north of 60°N to 3 m (Pg)	Integrated net CO_2 flux 1860–2100 due to:		
					CO_2 (Pg)	CO_2+climate change (Pg)	Climate change (Pg)
Control	Standard ORCHIDEE + vertical discretization of soil carbon; improved snow insulation and ice latent heat		191	211	−69	−68	1
Freeze	Control + inhibition of soil C decomposition when frozen	Frozen respiration function (see Fig. S2 for functions tested)	254	280	−81 + −2	−56 + −1	25 + −3
Permafrost	Freeze + insulation by SOM, vertical mixing of soil carbon, and yedoma	Cryoturbation diffusion constant k : .01 – .001 m^2/y	306	504	−88 + −1	−27 + −7	62 + −7
Heating	Permafrost + exothermic heat release with decomposition	Exothermic heat release H : 20–40 MJ/kg C	294	476	−80 + −2	4 + −18	85 + −16

Table S2. Influence of different terms of CH_4 budget

Increase of wetlands CH_4 emissions (Tg/y) in 2090–2100 in comparison to preindustrial emissions	CH_4 flux densities		Wetland extent	CO_2	CO_2+Climate	Climate
	Q_{10}	Soil carbon				
	3	F	F	+68	**+25**	−43
	3	F	PI	**+40**	**+83**	+43
	3	PI	F	+15	+19	+4
	3	PI	PI	+1	+59	+58
Increase of CH_4 emissions (Tg/y) linked to permafrost in comparison to preindustrial emissions	Permafrost case			0	+0.5	+0.5
	Heating case			0	+14	+14

CH_4 in ORCHIDEE arise from two separate submodels, a wetland source and a permafrost source. We apply different parameter and process sensitivities for the different sources, shown here as separate lines. The three columns on the right show the model high-latitude CH_4 emission changes (relative to a baseline of 33 Tg/y) due to changes in CO_2, total change due to CO_2 and climate, and the change due to climate alone (difference between first two columns). To assess the sensitivity of the CH_4 model to different processes, the model is run allowing the methanogenesis substrate to vary freely with the climate or to stay fixed (F) at preindustrial (PI) values. Separate F and PI runs are also done with the wetland extent. The three bold numbers refer to the panels in Fig. 4. T_{mean} is held constant for all the experiments listed here.